Research Square

Preprints are preliminary reports that have not undergone peer review.
They should not be considered conclusive, used to inform clinical practice,
or referenced by the media as validated information.

A Wearable IDC-Based Capacitive Sensing Belt for Real- Time Respiratory Monitoring and Weekly Athletic Performance Evaluation

Junaid Saddiqi

25020243@siswa.unimas.my

Universiti Malaysia Sarawak

Kasumawati Binti lias

Universiti Malaysia Sarawak

Muzamil Ayoub

Universiti Malaysia Sarawak

Research Article

Keywords: Interdigital capacitive, Polyethylene terephthalate, Respiratory rate, Non-invasive, diaphragmatic motion

Posted Date: October 6th, 2026

DOI: https://doi.org/10.21203/rs.3.rs-10880181/v1

License: This work is licensed under a Creative Commons Attribution 4.0 International License.
Read Full License

Additional Declarations: No competing interests reported.

A Wearable IDC-Based Capacitive Sensing Belt for Real-Time Respiratory Monitoring and Weekly Athletic Performance Evaluation

Junaid Saddiqi[1],Kasumawati binti Lias [1]*, Muzamil Ayoub[1]*

[1] Faculty of Engineering, Universiti Malaysia Sarawak, 94300 Kota Samarahan, Sarawak, Malaysia
**E-mails: 25020243@siswa.unimas.my , lkasumawati@unimas.my*

***ABSTRACT**:*

The growing demand in professional sports for precise and continuous performance assessment, has highlighted respiratory rate (RR) as a critical indicator of exertion, fatigue, and training adaptation. However,existing RR monitoring systems face limitations both in dynamic and static conditions due to reduced wearability, signal artifacts during motion, limited individual adaptability, and challenges in extracting reliable self referential and feedback oriented output. To address these limitations, a wearable interdigital capacitor (IDC) based smart belt is developed for the real time RR monitoring and longitudinal performance evaluation. The flexible IDC sensor is fabricated by a cost effective, screen printing technique on a Polyethylene terephthalate (PET) substrate using carbon conductive ink, The sensing mechanism captures capacitance variations induced by diaphragmatic motion through modulation of fringing electric fields. A robust signal conditioning strategy based on adaptive thresholding is employed to isolate true respiratory cycles from motion induced disturbances, ensuring reliable operation during dynamic activities.The proposed system includes an embedded acquisition unit and a custom designed software for real time visualization, detecting the RR pattern, and providing user friendly feedback. Experimental evaluation of the proposed sensor demonstrates a sensitivity of 1.1846 pF/N, corresponding to an estimated pressure sensitivity of ~1.036 pF/kPa, along with high linearity (R^2 = 0.98561), low hysteresis, and excellent repeatability, validated through a 500-second continuous respiratory signal showing stable and consistent breathing patterns, which means that the sensors work reliably. The system accurately monitors breathing patterns at different exercise intensities and implements a referential system that can obtain data in real time and generate a weekly assessment framework to measure respiratory adaptation through both endpoint and averaged metrics. The proposed platform provides a non-invasive, user specific, and feedback driven solution for continuous respiratory monitoring, offering practical utility in sports performance optimization.

Keywords : Interdigital capacitive ; Polyethylene terephthalate;Respiratory rate ; Non-invasive; diaphragmatic motion

I. INTRODUCTION

The Respiratory rate(RR) , is a critical parameter that needs to be continuously monitored across various pathological conditions[1], [2] .In healthcare, RR is a powerful predictor for early patient deterioration [3] and cardiac arrest [4], and it serves as an early indicator of hypoxia[5], hypercapnia[6], as well as metabolic and respiratory acidosis [7]. Despite its critical role in detecting patient deterioration, RR is the frequently monitored or automated vital sign, especially in medical and surgical wards[8]. Moreover, RR is sensitive to a range of stressors, such as emotional stress [2], Prolonged stress has been linked to immune system dysfunction [9], psychiatric conditions including anxiety, depression, and Alzheimer's disease[10],The World Health Organization (WHO) has even labeled stress as the health epidemic of the 21st century[11]. During exercise, RR serves as a reliable indicator of physical exertion and fatigue[12], [13], [14]. RR parameters are valuable in almost all sports related activities, as they reflect respiratory exchanges, the perception of fatigue particularly during prolonged endurance activities[15] and adaptations to training. Continuous monitoring of RR can also help prevent overtraining[16], making it a useful tool for assessing athletic performance. Professional sports increasingly demand advanced tools for performance assessment, as this area has become a rapidly expanding field within sports science. The primary goals are to prevent injuries, enhance athletes' responses to training and prevent overtraining. Consequently, obtaining reliable data that can be translated into practical guidance for coaches, trainers, and nutritionists has become critically important[17], [18].

As discussed earlier, there is a growing need for such systems that can monitor respiratory parameters and turn this data into useful actionable guidance for coaches, trainers, and athletes. Traditionally, respiratory monitoring in both clinical and sports settings has relied on tools such as spirometers[19], pneumotachographs[20], chest straps[21], and electrocardiography-based systems. While these traditional devices provide accurate measurements in controlled settings, they have significant drawbacks, including limited mobility, discomfort during long use, high costs, and the inability to enable continuous or real time monitoring during active physical activities. These issues make them less practical for daily training routines and long term performance evaluations. To overcome these limitations, and to monitor the RR , recent advancements in wearable sensing technology have made it possible to monitor respiratory and other essential physiological parameters continuously and in real-time. Modern wearable sensors[22], including capacitive[23], resistive[24], Magnetic Induction[25], piezoelectric[26], Bioimpedance Sensors [25], Inertial Sensors[25] have been widely explored for real-time respiratory monitoring. The application of these sensors for continuous respiratory monitoring has undergone comprehensive examination, revealing novel methodologies across various studies ,Such as Jiseon K et al.presented a study in which they uses an embroidered textile based capacitive sensor to measure breathing signals during different human motions and classifies them using a 1D CNN but this system have some sort of limitation like small dataset, controlled lab conditions, wired setup, and difficulty distinguishing similar motions like walking and light running[27]. Satoko H et al. – 2022 developed a wearable, flexible resistive based mask sensor that tracks respiration in real time by humidity changes but the system is limited by small volunteer testing, lack of clinical validation. Daniel T et al. – 2014 presents a textilebased magnetic induction sensor integrated in t-shirt that monitors respiration and pulse through four fabric-embedded magnetic eddy current sensors without direct skin contact but the system is sensitivity to posture and motion[28]. G. Roopa M et al. – 2013 presented The PVDF based piezo-electric nasal sensor detects respiration by converting airflow-induced bending near the nostrils into electrical

signals for real-time monitoring[29]. Chien-Lung S et al. – 2014 present smart bioimpedance based clothing system that monitor chest expansion and contraction to capture respiration signals non-invasively but the system is affected by motion artifacts by cloth and poor electrode contact[30]. Alessandra A et al. – 2023 present a system uses Inertial Measurement Unit sensor (IMUs) on the thorax, abdomen, and lower back to estimate respiratory rate during both static and dynamic activities.but the system is limited by small scale testing, sensitivity to motion artifacts as well [31].

Following the exploration of various sensing modalities for respiratory rate monitoring, it is evident that there is a significant need to address this issue in terms of feedback oriented ,personalized respiratory rate monitoring systems, sensitivity to motion artifacts and electrode contact .This is because most respiratory rate monitoring systems have been developed using general models or datasets obtained from multiple subjects. However, it is evident that effective respiratory rate monitoring in terms of healthcare and athletic performance requires systems that can be adapted to accommodate the individual characteristics of the subject under consideration. This again emphasizes the need to develop a self referential system that can obtain data in real time without relying on pre trained datasets. Moreover, to effectively address all of these challenges, there is a need to develop an intelligent sensing mechanism. In this context, sensor architectures such as an interdigital capacitor (IDC) can be used, as they provide flexibility due to their geometric configurations, which can be optimized to improve their sensing performance. These sensor architectures can thus provide better robustness in dealing with changes in the environment and motion induced disturbances. Besides hardware development, there is also a need to develop an intelligent software strategy to address motion artifacts as well as signal fluctuations. A threshold signal processing technique can be used to ensure that only physiologically significant signal patterns, which correspond to real breathing cycles, are detected, whereas all other signals, which could be due to body motion, are eliminated.

In this work, a wearable smart respiratory monitoring system is developed in the form of an IDC-based capacitive sensing belt. It is strategically designed to be placed over the diaphragmatic region in accordance with human anatomical considerations, thereby addressing the limitations identified in previous studies, as summarized in Table S1. The sensor is encapsulated using appropriate materials to minimize direct skin contact and reduce signal disturbances caused by external factors such as clothing and body motion. The sensing unit is integrated with a custom designed software interface, enabling real time visualization of respiratory activity through a user friendly web-based application. In order to improve the accuracy of the measurements, a threshold based signal processing algorithm is utilized to effectively differentiate between inhalation and exhalation, along with the elimination of motion artifacts and noise. However, the main advantage of the proposed system is its focus on personal monitoring, where continuous data collection is performed and recorded to enable future analysis. The system is designed to track the respiratory rate of the user during exercise and provide a weekly performance report, enabling the user to track the improvement in the respiratory patterns. Furthermore, the system includes a user friendly feedback mechanism, where the respiratory conditions are displayed using color coded markers on the animated human figure (male/female). Overall, the proposed system provides a non-invasive, adaptive, and user centric solution for real time respiratory monitoring and athletic performance evaluation, bridging the gap between wearable sensing, intelligent signal processing, and practical training feedback systems.

II. MATERIAL AND METHODS

I. Sensor Design and Fabrication

The IDC based flexible sensor was fabricated using a cost effective and scalable screen printing technique. The sensor geometry was first designed in CorelDRAW, with particular focus on optimizing the interdigital electrode pattern. The electrode finger width, spacing, and overall layout were carefully adjusted to reduce inter electrode gaps and enhance capacitance sensitivity, as shown in Fig. 1(a). The sensor dimensions are as follows: L1 = 3.5 cm (overall height), L2 = 2.5 cm (overall width), L3 = 2 cm (IDC comb length), L4 = 0.4 cm (sub-comb length to minimize spacing and enhance electric field interaction), and S1 = 0.25 cm (spacing between combs). This refined electrode configuration ensures enhanced electric field interaction and improved responsiveness to mechanical deformation caused by diaphragmatic movement

Following the design phase, the sensor pattern was transferred onto a screen printing mask by the process of photolithography in which the design of the IDC sensor which is being already created using CorelDRAW is then printed on transparent film. A fine mesh screen is coated with photosensitive emulsion, and the transparent film is placed on top. When exposed to UV light, the emulsion is hardened, but where there is no film, there is no exposure. Washing the screen removes the non exposed emulsion, creating open spaces that match the design of the IDC sensor, where ink is then printed, A flexible polyethylene terephthalate (PET) sheet with a thickness of 100 µm – 150 µm was selected as the substrate because of its lightweight nature, mechanical flexibility, and suitability for wearable applications. The prepared screen, containing the IDC pattern, was then aligned and placed over the PET substrate.Subsequently, conductive carbon ink paste was applied over the screen mask and spread uniformly using a squeegee to ensure proper deposition of the conductive ink onto the substrate. This step forms the IDC structure on the PET surface. The use of carbon based conductive ink not only provides adequate electrical conductivity but also maintains flexibility, making it ideal for wearable sensing application , Moreover it also generally more cost effective than many other conductive inks, especially silver-based inks.

After printing, the sensor was allowed to cure at a controlled temperature of approximately 60 °C for a fixed duration to ensure proper adhesion and stabilization of the conductive layer. This curing process enhances the mechanical integrity and electrical performance of the printed electrodes.The whole fabrication process is shown in Fig. 1(b). The fabricated IDC sensor was then integrated into a wearable belt shown in Fig. 1(c) intended for placement in the human diaphragmatic region. The wearable belt was designed to be sensitive to the expansion and contraction of the body. The sensor was then encapsulated in a 20 cm long packaging sheet with a thickness of 12.7 µm ,The encapsulation provides a complete seal, protecting the sensor materials from the surrounding environment and ensuring user safety by isolating trace residual chemicals. This prevents any risk of leaching, even during prolonged use or exposure to moisture. The final sensor assembly consists of a PET substrate with a carbon ink sensing layer, covered by a 12.7 µm thin packaging sheet. The total device thickness is approximately 275–395 µm, maintaining flexibility and durability.

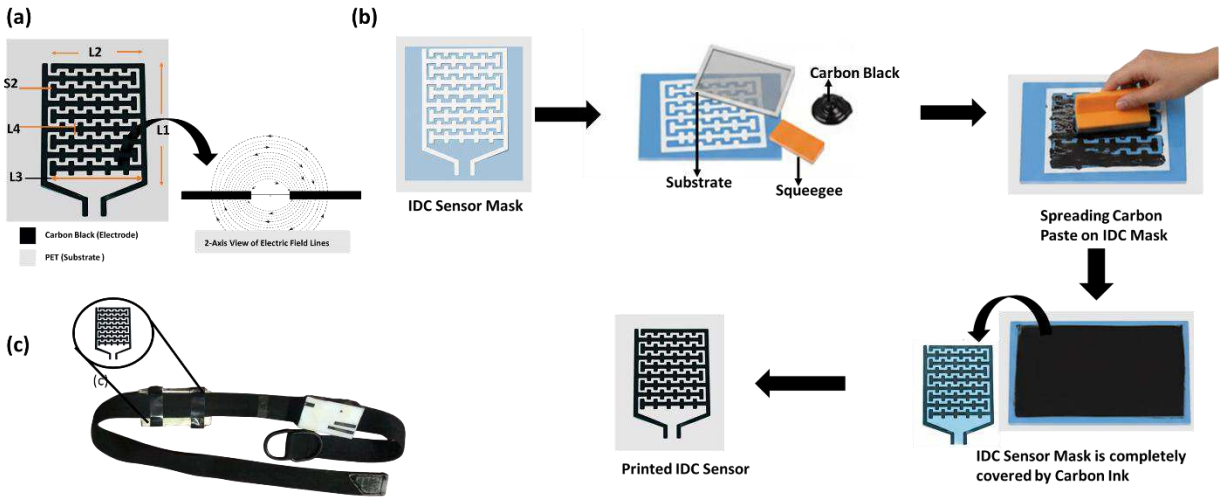


Fig. 1(a) Refined inter electrode configuration designed to enhance electric field interaction, resulting in improved sensitivity and responsiveness to mechanical deformation. (b) Schematic illustration of the overall fabrication process of the sensor, including pattern design, material deposition . (c) Printed sensors are embedded in the belt.

II. Characterization Setup

The IDC-based capacitive respiratory sensor was integrated with an Arduino Nano development board for real time data acquisition. The total capacitance of the sensor (C) is calculated using: $C = Cvc\ (N - 1)\ L$ [32], [33] Eq(1)

where Cvc is the capacitance of a single unit cell, N is the number of interdigitated electrodes, and L is the overlapping length of the electrodes. The unit cell capacitance consists of three components: $C1$ above the electrode surface, $C2$ between the electrodes, and $C3$ below the electrode surface: $Cvc = C1 + C2 + C3$ [32], [33] Eq(2)

The capacitances $C1$and $C3$are expressed as:

$$C1 + C3 = \varepsilon 0 \frac{(\varepsilon 1 + \varepsilon 3)}{2} \frac{k\sqrt{1-\left(\frac{g}{w}\right)^2}}{k(\frac{g}{w})} \quad [32], [33] \qquad \text{Eq(3)}$$

and $C2$ is expressed as:

$$C2 = \varepsilon 0\ \varepsilon 2\ (h / g) \quad [32], [33] \qquad \text{Eq(4)}$$

where $\varepsilon 0$ is the permittivity of free space, $\varepsilon 1, \varepsilon 2, \varepsilon 3$ are the relative permittivities above, between, and below the electrodes, g is the electrode spacing, w is the width of a single unit cell, h is the electrode thickness, and K(g/w) is the complete elliptical integral of the first kind. integral, g is the electrode spacing, w is the width of a single unit cell, and h is the electrode thickness or height. For IDC sensors, fringing electric field lines (FFLs) are significant since they extend beyond the edges of the electrodes. Moreover, in IDCs, if the spacing between electrodes is small, then the capacitive response is dominated by the FFLs. Therefore, any variation in the dielectric properties in the region of fringing electric field lines is considerable. For the proposed system, during the cyclic movement of the diaphragm due to breathing,

there is modulation in the dielectric properties in the region of FFLs. During exhalation, the diaphragm moves up and expands towards the IDC sensor as shown in Fig. 2(a). This is because, during exhalation, there is an increase in the permittivity in the region of fringing electric field lines, which in turn increases the capacitance. During inhalation, the diaphragm contracts and moves away from the IDC sensor as shown in Fig. 2(b). This is because, during inhalation, there is a decrease in permittivity in the region of fringing electric field lines, which in turn decreases the capacitance, Consequently the capacitance would be:

$$C = C0 + C\,resp \quad [33], [34] \qquad \text{Eq(5)}$$

where $C0$ is the baseline capacitance in free space and $C\,resp$ is the additional capacitance induced by diaphragmatic motion. Capacitance is directly proportional to the permittivity of the dielectric medium εr and inversely propotional to the (d) which is the separation between the electrode fingers:

$$C = \varepsilon 0\ \varepsilon r\,(A / d) \quad [33], [34] \qquad \text{Eq(6)}$$

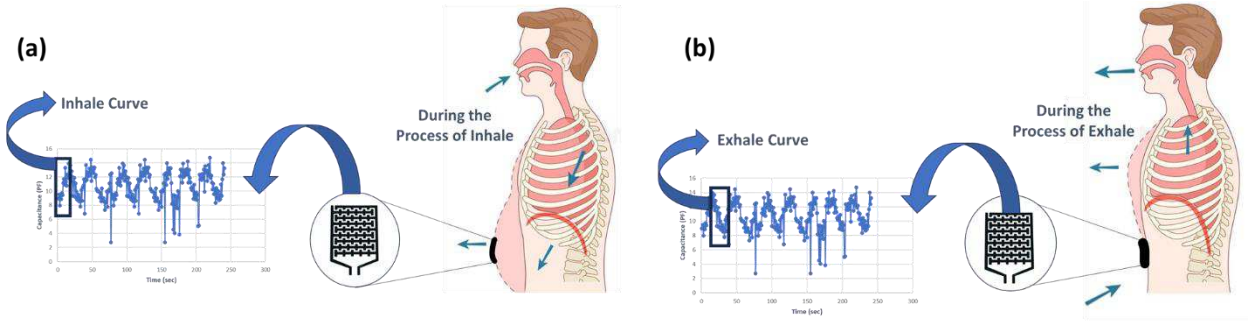


Fig. 2(a) Inhalation phase showing diaphragm contraction and corresponding sensor response curve. (b) Exhalation phase illustrating diaphragm relaxation with the associated sensor output curve.

For real time monitoring and analysis, the IDC sensor was connected to a custom designed software platform developed in Python. The capacitance data collected from the Arduino Nano was sent to the designed software using the Bluetooth Module HC-05 connected to the Arduino board and processed instantly. The processed signal was displayed through a graphical user interface (GUI), allowing for continuous tracking of breathing patterns. To ensure accurate detection of breathing cycles, a threshold based signal processing algorithm is used. Upper and lower threshold limits are defined to tell apart the exhalation and inhalation phases. The upper threshold marks the exhalation phase, where capacitance increases, while the lower threshold indicates the inhalation phase, where capacitance decreases. This method effectively reduces the effect of motion artifacts, noise, and unwanted fluctuations, ensuring that only relevant breathing signals are considered. A respiration cycle is defined as one complete inhalation and exhalation event. A counter is included to calculate the respiratory rate in real time. The system also gives visual feedback through dynamic graph plotting and an interactive display, where sensor readings appear on an animated human model (male or female) as selected by the user . The sensor region changes color based on set threshold levels, giving clear insight into breathing conditions,such as green indicates

a normal and stable breathing condition, where the signal lies within the optimal threshold range. Orange represents a moderate or transitional state, typically observed when the signal approaches the predefined thresholds, indicating slight irregularities or increased breathing effort. In contrast, red corresponds to a critical or abnormal condition, where the signal exceeds the upper threshold or falls below the lower threshold, suggesting rapid breathing, irregular patterns. Fig. 3 presents and explains the complete software interface of the proposed system.

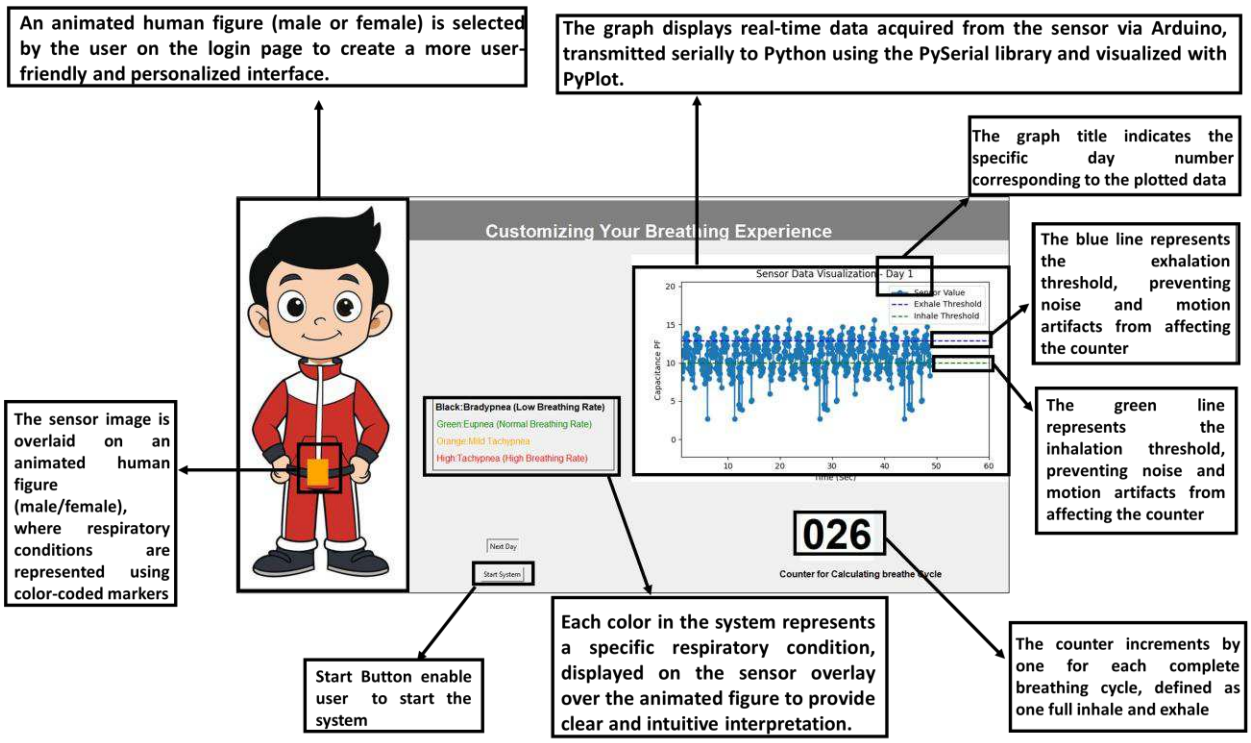


Fig. 3. illustrates the developed graphical user interface of the proposed respiratory monitoring system, where real-time data acquired from the IDC-based sensor is visualized alongside threshold-based inhale and exhale detection. The interface integrates a dynamic plot, a breathing cycle counter, and an animated human model with a sensor overlay to provide intuitive, color-coded feedback corresponding to different respiratory conditions.

To assess the athlete's respiratory performance over one week in controlled conditions (constant speed and duration), we recorded the breathing rate (BR) daily. initially quantified using the net percentage change between the first and last day, expressed as:

$$Weekly\ Improvement\ (\%) = \frac{BRday1 - BRday7}{BRday1} \times 100 \qquad \text{Eq(7)}$$

While this equation provides a straightforward indication of performance change, it does not account for day to day performance in breathing patterns. Therefore, to obtain a more accurate and reliable assessment, the average breathing rate over the week was also considered, calculated as:

$$BRavg = \frac{BR1 + BR2 + \cdots + BR7}{7} \qquad \text{Eq(8)}$$

An additional improvement metric was then defined using the weekly average:

$$Weekly\ Improvement\ (\%) = \frac{BRday1 - BRavg}{BRday1} \times 100 \qquad \text{Eq(9)}$$

This includes all recorded values and lessens the impact of brief fluctuations. A consistent drop in breathing rate, shown in both end-point and average-based evaluations, indicates improved cardiorespiratory efficiency. The athlete needs fewer breaths to maintain the same workload. This combined method ensures a more thorough and reliable evaluation of respiratory adaptation over time. Fig. 4 presents the overall characterization setup of the proposed respiratory monitoring system .

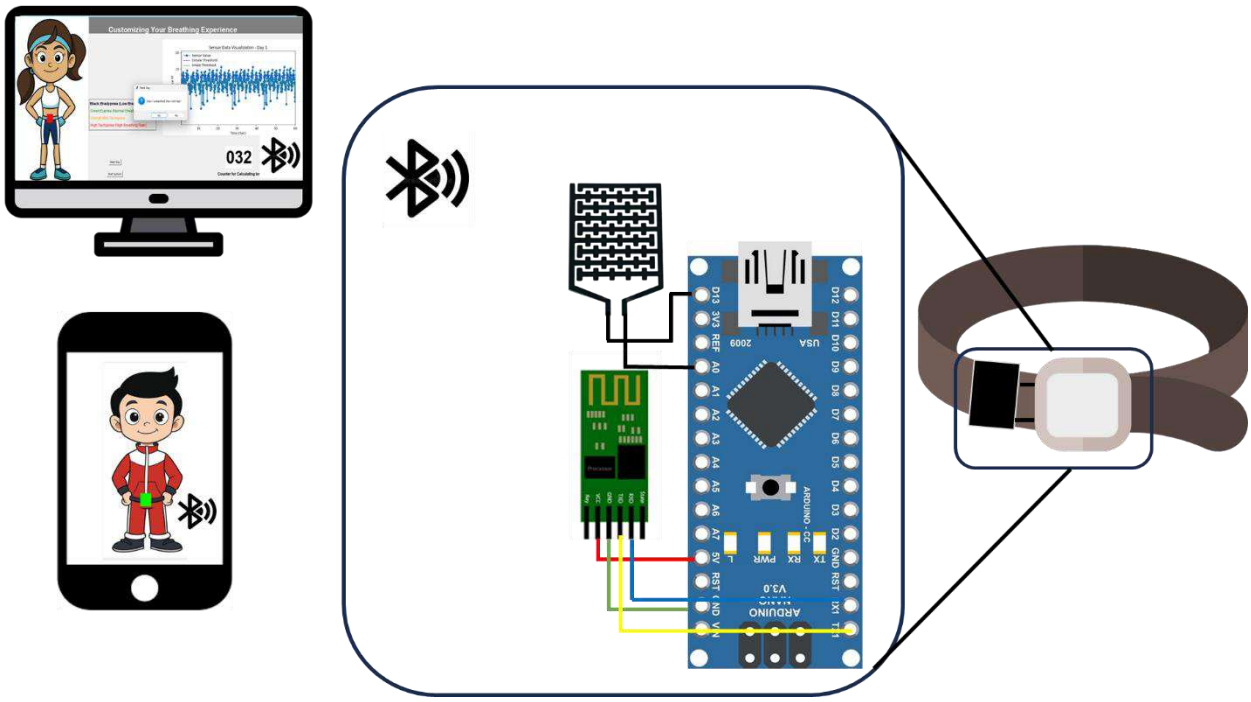


Fig. 4. illustrates the developed graphical user interface of the proposed respiratory monitoring system, where real-time data acquired from the IDC-based sensor is visualized alongside threshold-based inhale and exhale detection. The interface integrates a dynamic plot, a breathing cycle counter, and an animated human model with a sensor overlay to provide intuitive, color-coded feedback corresponding to different respiratory conditions.

III. RESULTS AND DISCUSSION

The proposed IDC based respiratory sensing system was tested through a detailed experimental analysis. This included sensor characterization, real-time respiratory monitoring during different physical activities, and a software-based feedback assessment.

First, the sensor characterization aimed to confirm its effectiveness for respiratory monitoring. The linearity of the sensor[35] was checked by fitting the experimental data to the linear equation:

$$Y = mX + c \quad [36] \qquad \text{Eq(10)}$$

where $Y$and X represent the fitted capacitance and applied stimulus (e.g., diaphragm displacement or simulated weight), respectively, *m* represents the sensitivity and *c* is the intercept, which is being calculated as :

$$m = \frac{n.sumxy - sumx.sumy}{n.sumx2 - (sumx)2} \qquad \text{Eq(11)}$$

$$c = \frac{sumy - m.sumx}{n} \qquad \text{Eq(12)}$$

The values chosen for *m* and *c* variables are derived from the input weights for our proposed system the value of *m* is 1.1846 and value of *c* is 12.3363 and overall sum of square residual is 1.6901, which is relatively very small indicating that the model predictions are closer to the actual data, meaning a better fit,Similarly the high coefficient of determination (R^2 = 0.98561) indicates excellent linearity, demonstrating that the sensor provides consistent and predictable capacitance responses, making it highly reliable for applications such as respiratory rate monitoring. Additionally, the hysteresis analysis [37] revealed minimal differences between the loading and unloading cycles. This confirms low hysteresis loss and excellent repeatability of the sensor. The effective sensing area of the fabricated IDC sensor is approximately 3.5 cm × 2.5 cm . Based on the slope of the linear fit (1.1846 pF/N), the estimated pressure sensitivity of the sensor is approximately 1.036 pF/kPa.These features ensure stable and accurate measurements . The Hysterisis and linearity curve of our proposed system is shown in Fig. 5 (a) and (b).

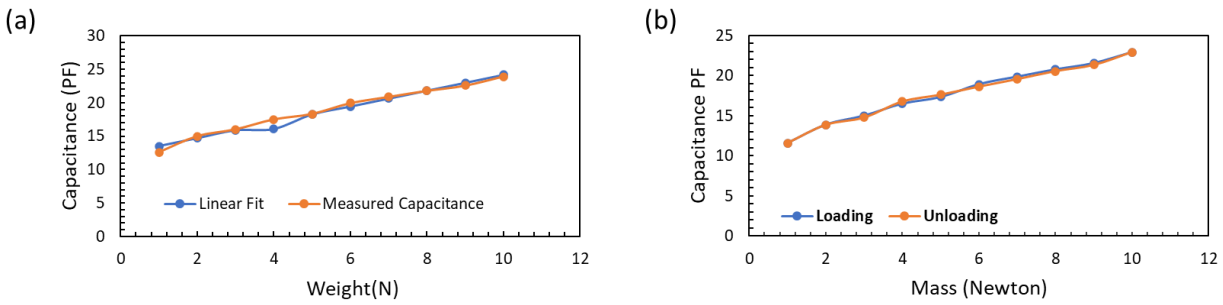


Fig. 5. Characteristics of the fabricated IDC senso for respiratory rate monitoring (a) Linear relationship between applied weight (N) and measured capacitance (pF), and (b) Hysteresis behavior showing capacitance variation (pF) during loading and unloading of weight (N).

To further validate the sensor's performance under varying conditions, the respiratory belt was placed on an individual, and respiratory data were recorded during physical activities of different intensities. Breathing rates were monitored during light, moderate, and intense exercise performed on the same day. Before integrating the data into our custom software, the sensor output was streamed directly to Excel using the data streamer , which directly plot the Arduino data on the excel for real time plotting. The results show that respiratory rate increases with physical exertion, clearly reflected in the inhalation and exhalation spikes as shown in Fig. 6 This trend confirms the sensor's capability to detect changes in breathing patterns, with real time graphs showing consistent and distinct inhale exhale cycles, demonstrating reliable operation even during motion and varying physiological conditions. Similarly, respiratory signals were recorded for an extended duration of approximately 500 seconds to evaluate the long-term stability and performance of the sensor, particularly its susceptibility to noise and motion artifacts. The results are presented in Supplementary Fig. S1.

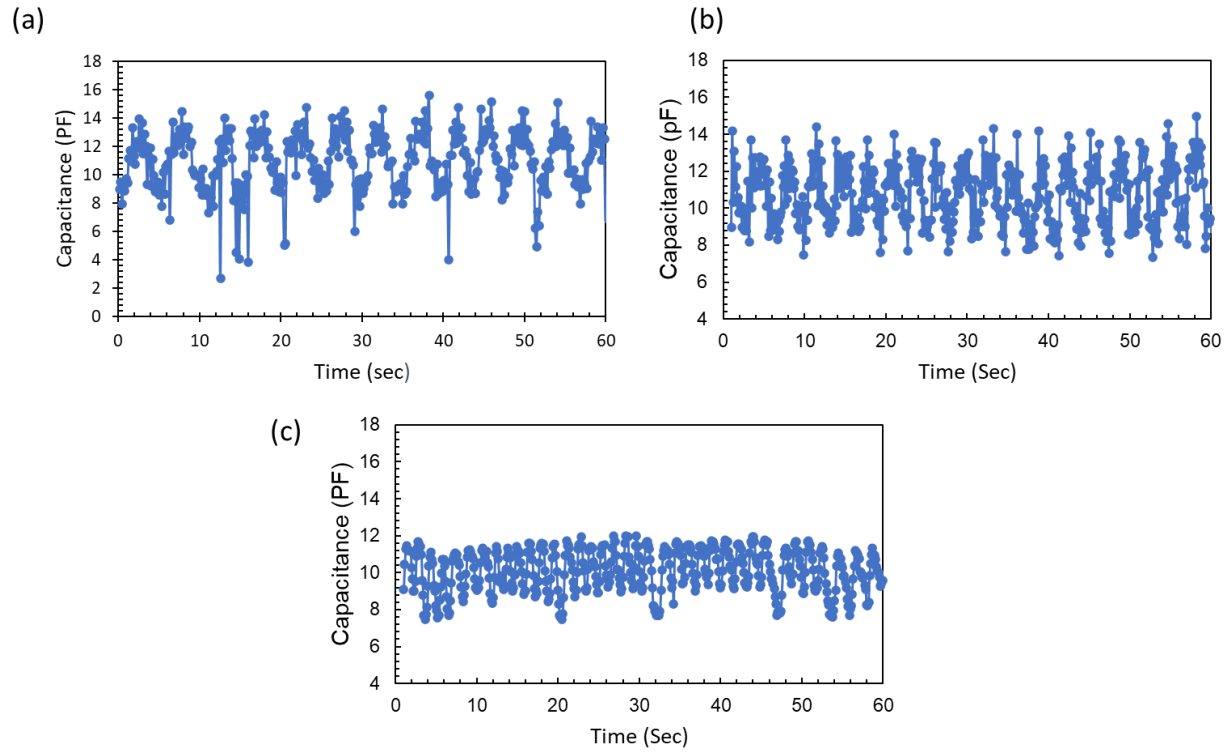


Fig. 6. Assessment of the sensor's performance under different activity levels: (a) Respiratory rate during light exercise, (b) Respiratory rate during moderate exercise, and (c) Respiratory rate during high-intensity exercise.

Following the validation of the sensor's performance, a custom software interface was developed to enable real time visualization and analysis of the respiratory activity in real time . The software starts with a user authentication and data input process, as shown in Fig. 7(a). In this process, the user is required to enter basic details such as name, gender, and level of activity (speed). Moreover, the gender of the user can be set to either male or female, which automatically adjusts the graphical interface with the corresponding male or female animated model,In addition, the level of activity of the user is taken into account as a reference parameter while assessing the weekly respiratory performance of the user. One of the important aspects of the interface is the implementation of a color coded system of respiratory

classification according to the physiological rates of breathing. This system is implemented based on the physiological rates of breathing and can classify the states of breathing into three main states: low breathing rates (bradypnea), normal breathing (eupnea), and high breathing rates (tachypnea). Each of these states of breathing is represented by a specific color code. These color code is implemented on the positions of the sensors on the animated model of the human body, as shown in Fig. 7(b).

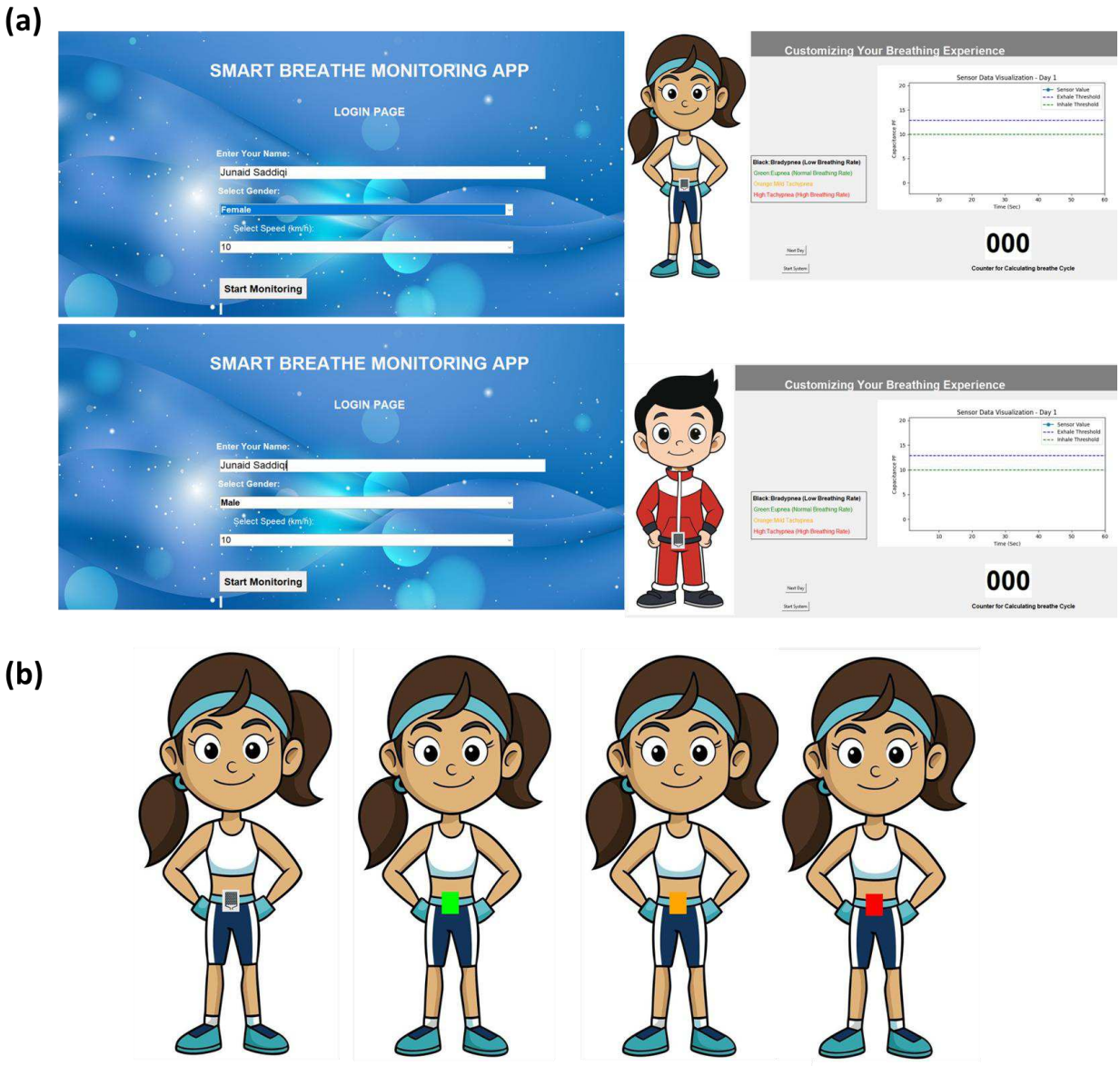


Fig. 7. Graphical user interface (GUI) of the proposed smart respiratory monitoring system: (a) User login interface with gender-based personalized display (male/female).(b) Real-time monitoring interface with threshold-based respiration tracking and color-coded breathing conditions (green, orange, red).

For ensuring an accurate respiratory cycle, a threshold based signal processing algorithm was also included. The incoming signal is continuously monitored, and the thresholds for inhaling and exhaling are used to filter the actual respiratory cycles and distinguish them from any unwanted signals or movements.

The exhaling threshold also acts as a boundary for the system to prevent false triggers that may occur due to minor changes or movements. The entire respiratory cycle, including both inhaling and exhaling, is counted through a digital counter, and the actual rate can be computed in real time. The success of this approach is also evident through the real time plots shown in Fig. 8, where clear respiratory cycles are evident.The system is also designed to track the performance over a longer time. The system is capable of collecting and storing respiratory signals for a week, and each day's recorded values are available for visualization through a separate interface, as shown in Fig. 8.

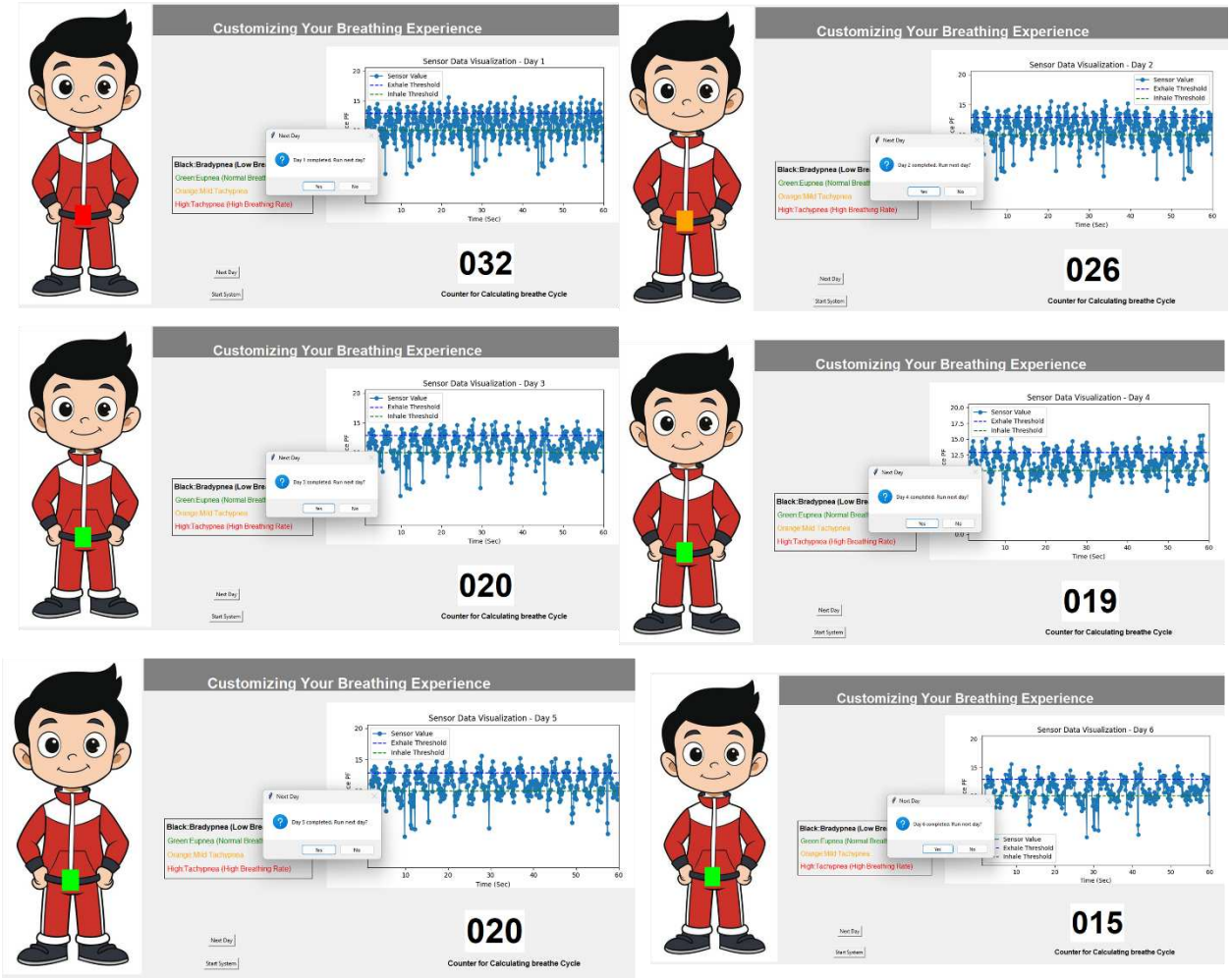


Fig. 8. Day-wise respiratory monitoring from Day 1 to Day 6, showing real-time sensor data, breathing cycle counts, and color-coded respiratory conditions, illustrating progressive changes in breathing patterns over time.

At the end of the monitoring period, a weekly performance evaluation report will be generated, as represented in Fig. 9. The report will contain daily and overall evaluations, indicating improvements or deviations in respiratory rate. The evaluation will be carried out using end point comparison between Day 1 and Day 7, and average values, making it a reliable approach for assessing respiratory adaptation. The final report will be useful, having graphical representation and performance indicators, making it suitable for personal and medical use.



Fig. 9. Final day (Day 7) respiratory monitoring and system-generated weekly performance evaluation, showing real-time sensor data with threshold detection and the summarized report of breathing rate improvement over the 7-day period.

.

IV. CONCLUSION

This study presents the design and development of an IDC-based capacitive respiratory monitoring system integrated within a wearable belt for real time and personalized breathing analysis. The proposed sensor demonstrated excellent performance characteristics, including high linearity ($R^2 = 0.98561$), low hysteresis, and stable repeatability. The proposed system is, therefore, suitable for continuous monitoring of respiratory patterns. The experimental results, conducted while changing physical activity levels, show that the system is effective in monitoring respiratory patterns, as the rate of breathing is proportional to the intensity of physical activity. In addition to hardware performance, the proposed system directly addresses key limitations of existing respiratory monitoring approaches, especially the lack of

personalization, motion artifacts, and the use of generalized models. Unlike the existing techniques, the proposed system is based on the concept of self referential, as the system is designed to perform user specific analysis. The threshold based algorithm reduces motion and environmental noise, ensuring precise detection of inhalation and exhalation cycles without reliance on complex electrode contact mechanisms. The custom designed software interface provides an opportunity to visualize the respiratory patterns in real time, as indicated by the color codes, and the analysis of the respiratory cycles, as well as the weekly performance report, helps in the monitoring and evaluation of the respiratory patterns over time. Overall, the proposed system provides a low-cost, non-invasive, and scalable solution that overcomes critical challenges in existing methods while offering reliable, personalized respiratory monitoring.

Acknowledgment.

The authors would like to acknowledge the support provided by Supervisor , Universiti Malaysia Sarawak

Disclosures. The authors declare no conflicts of interest.

Data availability.

The data supporting this study's findings are available from the corresponding authors upon reasonable request.

Funding.

This manuscript has been conducted without any external financial support or funding from any organization. The authors declare that no funding was received for the research, authorship, or publication of this work

Author Contribution.

Junaid Saddiqi conceived the project idea, designed the data collection system/software, and prepared the original manuscript draft. Muzamil Ayoub contributed to data collection and assisted in rewriting and editing the manuscript. Kasumawati Binti Lias supervised the overall project and provided guidance in idea development, formulation, and structural organization of the study

Clinical Trial Registration: Not applicable. This study was not a clinical trial and no clinical trial registration was conducted.

Ethics, Consent to Participate, and Consent to Publish: The experimental testing was conducted solely by the author as a self-assessment study. No other human participants were involved. Therefore, formal participant consent and ethics approval were not applicable.

REFERENCES

[1] A. Nicolò, C. Massaroni, and L. Passfield, "Respiratory Frequency during Exercise: The Neglected Physiological Measure," *Front. Physiol.*, vol. 8, Dec. 2017, doi: 10.3389/fphys.2017.00922.

[2] A. Nicolò, C. Massaroni, E. Schena, and M. Sacchetti, "The Importance of Respiratory Rate Monitoring: From Healthcare to Sport and Exercise," *Sensors*, vol. 20, no. 21, Nov. 2020, doi: 10.3390/s20216396.

[3] M. M. Churpek, T. C. Yuen, and D. P. Edelson, "Predicting clinical deterioration in the hospital: The impact of outcome selection," *Resuscitation*, vol. 84, no. 5, pp. 564–568, May 2013, doi: 10.1016/j.resuscitation.2012.09.024.

[4] "The Medical Journal of Australia".

[5] "Overview of Hypoxia around the World - Diaz - 2001 - Journal of Environmental Quality - Wiley Online Library." Accessed: Mar. 29, 2026. [Online]. Available: https://acsess.onlinelibrary.wiley.com/doi/abs/10.2134/jeq2001.302275x

[6] "Hypercapnia | New England Journal of Medicine." Accessed: Mar. 29, 2026. [Online]. Available: https://www.nejm.org/doi/abs/10.1056/NEJM198911023211804

[7] S. Rolfe, "The importance of respiratory rate monitoring," *Br. J. Nurs.*, vol. 28, no. 8, pp. 504–508, Apr. 2019, doi: 10.12968/bjon.2019.28.8.504.

[8] C. H. Van Leuvan and I. Mitchell, "Missed opportunities? An observational study of vital sign measurements," *Crit. Care Resusc.*, vol. 10, no. 2, pp. 111–115, Jun. 2008, doi: 10.1016/S1441-2772(23)01322-4.

[9] "Stress-induced immune dysfunction: implications for health | Nature Reviews Immunology." Accessed: Mar. 29, 2026. [Online]. Available: https://www.nature.com/articles/nri1571

[10] A.-M. Bao, G. Meynen, and D. F. Swaab, "The stress system in depression and neurodegeneration: Focus on the human hypothalamus," *Brain Res. Rev.*, vol. 57, no. 2, pp. 531–553, Mar. 2008, doi: 10.1016/j.brainresrev.2007.04.005.

[11] A. Hernando *et al.*, "Inclusion of Respiratory Frequency Information in Heart Rate Variability Analysis for Stress Assessment," *IEEE J. Biomed. Health Inform.*, vol. 20, no. 4, pp. 1016–1025, Jul. 2016, doi: 10.1109/JBHI.2016.2553578.

[12] "Comparing Continuous and Intermittent Exercise: An 'Isoeffort' and 'Isotime' Approach | PLOS One." Accessed: Mar. 29, 2026. [Online]. Available: https://journals.plos.org/plosone/article?id=10.1371/journal.pone.0094990

[13] "Respiratory frequency and tidal volume during exercise: differential control and unbalanced interdependence - Nicolò - 2018 - Physiological Reports - Wiley Online Library." Accessed: Mar. 29, 2026. [Online]. Available: https://physoc.onlinelibrary.wiley.com/doi/full/10.14814/phy2.13908

[14] A. Nicolò *et al.*, "A comparison of different methods to analyse data collected during time-to-exhaustion tests," *Sport Sci. Health*, vol. 15, no. 3, pp. 667–679, Dec. 2019, doi: 10.1007/s11332-019-00585-7.

[15] "Adaptations Of Skeletal Muscle To Prolonged, Intense Endurance Training - Hawley - 2002 - Clinical and Experimental Pharmacology and Physiology - Wiley Online Library." Accessed: Mar. 29, 2026. [Online]. Available: https://onlinelibrary.wiley.com/doi/abs/10.1046/j.1440-1681.2002.03623.x
[16] G. Kenttä and P. Hassmén, "Overtraining and Recovery," *Sports Med.*, vol. 26, no. 1, pp. 1–16, Jul. 1998, doi: 10.2165/00007256-199826010-00001.
[17] "Maximizing Cellular Adaptation to Endurance Exercise in Skeletal Muscle: Cell Metabolism." Accessed: Mar. 29, 2026. [Online]. Available: https://www.cell.com/cell-metabolism/fulltext/S1550-4131(18)30257-2
[18] A. Di Paco and R. Cannataro, "Respiratory frequency: from health to sports performance monitoring," *Med. Gas Res.*, vol. 15, no. 2, p. 218, Jun. 2025, doi: 10.4103/mgr.MEDGASRES-D-24-00134.
[19] "Spirometry | Clinical Reviews in Allergy & Immunology | Springer Nature Link." Accessed: Mar. 29, 2026. [Online]. Available: https://link.springer.com/article/10.1007/s12016-009-8128-z
[20] "Design and calibration of unicapillary pneumotachographs | Journal of Applied Physiology | American Physiological Society." Accessed: Mar. 29, 2026. [Online]. Available: https://journals.physiology.org/doi/full/10.1152/jappl.1998.84.1.335
[21] G. Cosoli, S. Spinsante, and L. Scalise, "Wrist-worn and chest-strap wearable devices: Systematic review on accuracy and metrological characteristics," *Measurement*, vol. 159, p. 107789, Jul. 2020, doi: 10.1016/j.measurement.2020.107789.
[22] K. N. Vaishnav, R. P. Verma, and B. Saha, "Advancements in 3D-printed wearable sensors: a modern healthcare," *Mater. Today*, vol. 89, pp. 502–535, Oct. 2025, doi: 10.1016/j.mattod.2025.08.006.
[23] A. Tahir *et al.*, "E-waste Driven Interdigitated Capacitive Wearable Sensor for Breath Rate Monitoring Applications," *Sens. Imaging*, vol. 26, no. 1, p. 138, Oct. 2025, doi: 10.1007/s11220-025-00663-w.
[24] "A New Approach for Readout of Resistive Sensor Arrays for Wearable Electronic Applications | IEEE Journals & Magazine | IEEE Xplore." Accessed: Mar. 29, 2026. [Online]. Available: https://ieeexplore.ieee.org/abstract/document/6846335
[25] T. Hussain, S. Ullah, R. Fernández-García, and I. Gil, "Wearable Sensors for Respiration Monitoring: A Review," *Sensors*, vol. 23, no. 17, Aug. 2023, doi: 10.3390/s23177518.
[26] "A Flexible and Biodegradable Piezoelectric-Based Wearable Sensor for Non-Invasive Monitoring of Dynamic Human Motions and Physiological Signals - Ali - 2023 - Advanced Materials Technologies - Wiley Online Library." Accessed: Mar. 29, 2026. [Online]. Available: https://advanced.onlinelibrary.wiley.com/doi/full/10.1002/admt.202300347
[27] J. Kim and J. Kim, "Classification of Breathing Signals According to Human Motions by Combining 1D Convolutional Neural Network and Embroidered Textile Sensor," *Sensors*, vol. 23, no. 12, Jun. 2023, doi: 10.3390/s23125736.
[28] D. Teichmann, A. Kuhn, S. Leonhardt, and M. Walter, "The MAIN Shirt: A Textile-Integrated Magnetic Induction Sensor Array," *Sensors*, vol. 14, no. 1, pp. 1039–1056, Jan. 2014, doi: 10.3390/s140101039.
[29] G. Roopa Manjunatha, K. Rajanna, D. R. Mahapatra, M. M. Nayak, U. M. Krishnaswamy, and R. Srinivasa, "Polyvinylidene fluoride film based nasal sensor to monitor human respiration pattern: An initial clinical study," *J. Clin. Monit. Comput.*, vol. 27, no. 6, pp. 647–657, Dec. 2013, doi: 10.1007/s10877-013-9486-x.
[30] C.-L. Shen *et al.*, "Respiratory Rate Estimation by Using ECG, Impedance, and Motion Sensing in Smart Clothing," *J. Med. Biol. Eng.*, vol. 37, no. 6, pp. 826–842, Dec. 2017, doi: 10.1007/s40846-017-0247-z.

[31] A. Angelucci and A. Aliverti, “An IMU-Based Wearable System for Respiratory Rate Estimation in Static and Dynamic Conditions,” *Cardiovasc. Eng. Technol.*, vol. 14, no. 3, pp. 351–363, Jun. 2023, doi: 10.1007/s13239-023-00657-3.
[32] M. Adnan *et al.*, “IDC pressure sensors enabled smart footwear system for in vitro detection and monitoring of diabetic foot ulcer,” *Sens. Actuators Phys.*, vol. 388, p. 116489, Jul. 2025, doi: 10.1016/j.sna.2025.116489.
[33] A. Tahir *et al.*, “E-waste Driven Interdigitated Capacitive Wearable Sensor for Breath Rate Monitoring Applications,” *Sens. Imaging*, vol. 26, no. 1, p. 138, Oct. 2025, doi: 10.1007/s11220-025-00663-w.
[34] M. Q. Mehmood *et al.*, “Lithography-Based Fabricated Capacitive Pressure Sensitive Touch Sensors for Multimode Intelligent HMIs,” *IEEE Access*, vol. 11, pp. 127411–127421, 2023, doi: 10.1109/ACCESS.2023.3332165.
[35] N. K. Vitanov and Z. I. Dimitrova, “Simple Equations Method and Non-Linear Differential Equations with Non-Polynomial Non-Linearity,” *Entropy*, vol. 23, no. 12, Dec. 2021, doi: 10.3390/e23121624.
[36] Z. Liaqat, J. Saddiqi, M. Q. Mehmood, M. Zubair, M. A. Imran, and Q. H. Abbasi, “Capacitive Pressure Sensitive Smart Shoe Insole for Gait Improvement of Cerebral Palsy Patients,” in *2025 IEEE International Symposium on Antennas and Propagation and North American Radio Science Meeting (AP-S/CNC-USNC-URSI)*, Jul. 2025, pp. 2204–2207. doi: 10.1109/AP-S/CNC-USNC-URSI55537.2025.11266285.
[37] “What is Hysteresis? | Appl. Mech. Rev. | ASME Digital Collection.” Accessed: Apr. 01, 2026. [Online]. Available: https://asmedigitalcollection.asme.org/appliedmechanicsreviews/article-abstract/64/5/050801/369998/What-is-Hysteresis

Supplementary Files

This is a list of supplementary files associated with this preprint. Click to download.

- SupplementaryInformation.docx